CrossMark

Seismic behavior of concentrically braced frames designed using direct displacement-based method

Dipti Ranjan Sahoo[1] · Ankit Prakash[2]

Abstract

This study is focussed on the evaluation of seismic performance of concentrically steel braced frames (CBFs) designed using direct displacement-based (DDBD) method. Design displacement profile in this method is derived from the inelastic mode shape normalized based on first story displacement. Design base shear of a structure is determined using design displacement spectrum and the equivalent viscous damping. Two low- and medium-rise CBFs, namely, 3-story and 6-story, are designed using DDBD method as well as current practice. These study frames are modelled and analysed in a computer software *OpenSEES* to compare their seismic performance under a set of selected ground motions. Braces are modelled using force-based fibre-discretized non-linear beam-column elements simulating the effects of inelastic buckling, large strain and low-cycle fatigue. The main parameters investigated are the maximum story displacements, the interstory drifts, the residual drifts and the yield mechanisms. DDBD frames exhibited the improved seismic response as compared to those design as per current practice.

Keywords Concentrically braced frame · Nonlinear dynamic analysis · Seismic analysis · Seismic design

1 Introduction

Steel concentrically braced frames (CBFs) are considered as one of the cost-effective lateral force-resisting systems, especially in low- and medium-rise buildings. The convenience of performing design or at least, checks by hand, also makes them less vulnerable to computational and modelling errors. Erection of CBFs is easier due to the fact that mostly they involve simple beam-column shear connections and this even reduces number of key elements to be verified during field inspection. Despite above advantages, CBFs are not preferred as the first choice for earthquake load-resisting systems in high-seismic regions (Tremblay 2002). This is primarily due to limited energy dissipation potential in compression due to severe pinching of hysteretic curve and buckling of steel braces and pre-mature low-cycle fatigue fracture of braces. Being short-period stiffer systems, the braced frames (especially, low-rise) respond in the "constant spectral acceleration" range (Chopra 1995) resulting in the higher displacement response. Also, the inelastic dynamic response of short-period structure is more sensitive to the shape of hysteretic curves, thus making the seismic behavior of CBFs to be relatively complicated.

The evolution of seismic design of structures started with concept of mass proportional lateral forces and further developed with adoption of structural period effect on inertia forces and incorporation of ductility considerations with somewhat arbitrarily reduced seismic force levels and elastic analysis of structures. Force-based design procedure does not guarantee in achieving the desired performance objectives by mere reduction of seismic forces (Ghobarah 2001). It has been realized that deformations, not strength, can be directly related to damage potential, which led to the development of performance-based design framework. This design philosophy aims at achieving the pre-determined performance goals for a structure subjected to the specified levels of seismic events.

Different approaches have been introduced to achieve the performance objectives in the performance-based seismic design framework. In the N2 method proposed by Fajfar and Gašperšič (1996), the seismic displacement demand

✉ Dipti Ranjan Sahoo
   drsahoo@civil.iitd.ac.in

[1] Department of Civil Engineering, Indian Institute of Technology Delhi, New Delhi, India

[2] National Thermal Power Corporation Limited, New Delhi, India

estimated by response spectrum analysis of an equivalent single-degree-of-freedom (SDOF) bilinear model for first elastic mode is compared with push-over analysis results of the real multi-degree-of-freedom (MDOF) structure with an assumed displacement profile. This displacement demand is used to determine the local and global damage indices. Capacity spectrum method is similar to the N2 method with the difference that damage indices are not specifically referenced, and that seismic demand (expressed in terms of a response spectra set) and the capacity (expressed as a push-over curve of equivalent SDOF model) curves are plotted on the same graph with spectral acceleration and displacement represented on vertical and horizontal axes, respectively. Equivalent elastic damping is derived from the ductility demand. Fajfar (1998) made use of inelastic spectra and related capacity to displacement-ductility demand, rather than equivalent viscous damping. Goel and Chao (2008) proposed a performance-based plastic design method based on the energy balance concept, which directly incorporates the target drift and yield mechanism in the design. This method has been successfully applied to buckling-restrained braced frames (Sahoo and Chao 2010) and reinforced concrete structures (Sahoo and Rai 2013).

Both the N2 and capacity-spectrum methods are extension of force-based procedures with a displacement check to ensure that acceptable performance levels are achieved under the design earthquake (Priestley 2000). On the hand, direct displacement-based design (DDBD) procedure is an alternative approach in which structures are designed to achieve a specified strain or drift performance level under a specified seismic intensity (Priestley et al. 2007). DDBD procedure focusses on the displacement parameter, rather than force, as the direct indicator of performance or damage. Considering the inherent weakness of CBFs in terms of the unpredictable and adverse performance during large seismic events, the performance objectives are considered in terms of peak inter-story drift ratio, residual inter-story drift ratio and expected structural damage in terms of the low-cycle fatigue damage of braces, behavior of columns, beams and braces. The peak inter-story drift limits for CBFs are governed by brace fracture ductility considerations which essentially controls the extent of damage in the structure altogether (Kumar et al. 2015; Kumar and Sahoo 2016).

The development of DDBD procedure for CBF has been carried out by many researchers in the recent past (Della Corte and Mazzolani 2008; Wijesundara 2009; Goggins and Sullivan 2009; Salawdeh and Goggin 2012). The procedure developed by Wijesundara (2012) is based on classical DDBD approach by Priestley et al. (2007) and uses the EVD of the system based on brace slenderness ratio. This procedure appears to be most suitable for adoption in design process (Salawdeh and Goggin 2012; O'Reilly et al. 2012). Although the DDBD method has been used in CBFs

in achieving the desired design drift limits under earthquake ground motions, further evaluation of the design procedure is required in terms of comprehensive performance objectives. In this study, DDBD procedure has been developed for the design of two low- and medium-rise (i.e., 3-stroy and 6-story) CBF systems. The seismic performance of these frames is evaluated through nonlinear static and dynamics analyses and is compared with the counterparts designed based on the current code procedures. The main parameters investigated are the inter-story drift response, residual drift response, plastic rotations of frame members, and yield mechanism under design-basis earthquake (DBE) and maximum considered earthquake (MCE) hazard levels.

2 Direct Displacement-Based Design (DDBD) Method

DDBD method is conceptually based on a substitute structure method in which multi-degrees-of-freedom (MDOF) system is replaced by an equivalent single degree-of-freedom (SDOF) system as shown in Fig. 1a. In force-based seismic design, a structure is characterized by its elastic or pre-yield properties, i.e., initial stiffness, K_i and elastic damping. However, DDBD characterizes the structure through the effective secant stiffness, K_e of the system at the desired design displacement Δ_d (Fig. 1b). Equivalent viscous damping (EVD) for the substitute structure for a specified ductility is estimated based on hysteretic behavior as shown in Fig. 1c. Using EVD and design displacement set at the start of the design, effective period for the substitute structure is obtained using the scaled spectral displacement spectrum, as shown in Fig. 1d, for a given seismic hazard. Design base shear for the structure is computed based on the effective period by multiplying the effective lateral stiffness to the spectral displacement.

Thus, the design procedure for displacement-based methodology can be broadly divided into four broad steps: (1) evaluation of yield displacement profile of the MDOF system, (2) selection of design displacement profile of the structure, (3) the transformation of MDOF system into an equivalent SDOF system for the first inelastic mode of response, and (4) estimation of base shear using damped displacement spectrum for the appropriate equivalent viscous damping. These design steps are discussed in detail as follows:

2.1 Yield Displacement Profile

The lateral displacement at ith story a braced frame at the yielding stage can be computed considering the simultaneous buckling and yielding of braces at the story level. This yield displacement ($\Delta_{y,i}$) can be considered as the sum of displacements corresponding to the sway mechanism (Δ_{sy}) and
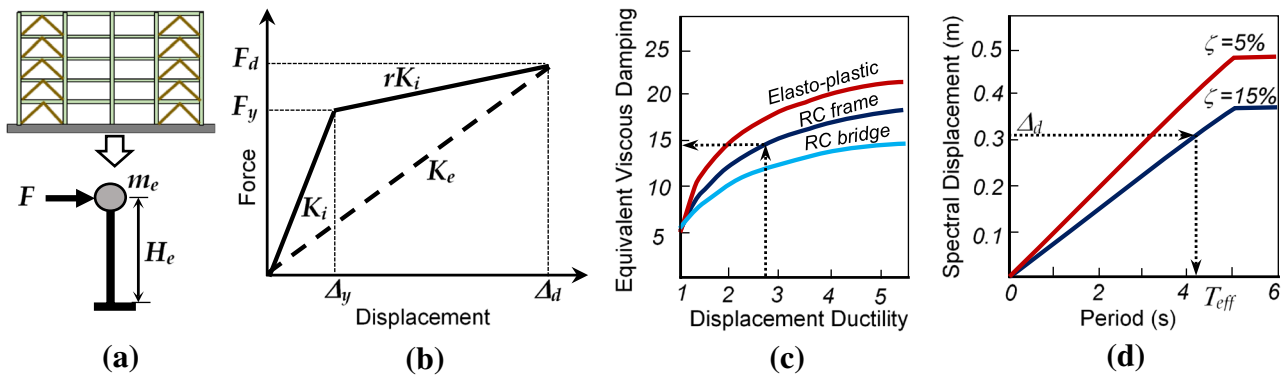
Fig. 1 Basic steps of direct displacement-based seismic design: **a** SDOF representation, **b** effective stiffness, **c** equivalent viscous damping, **d** displacement spectrum

the rigid-body rotation (Δ_{ry}) of the story as shown in Fig. 2. Accordingly, $\Delta_{y,i}$ can be expressed as follows (Wijesundara 2012):

$$\Delta_{y,i} = \Delta_{sy,i} + \Delta_{ry,i} = \left(\frac{2\varepsilon_y}{\sin 2\alpha}\right)h_i + \left(\beta\varepsilon_{yc}h_i\right)\tan\alpha \quad (1)$$

where $h_i = i$th story height, $\alpha =$ brace inclination angle with the horizontal (i.e., $\tan\alpha = 2h_i/B$), $\beta =$ ratio of design axial force to the yielding force of the column section, B = Bay width, ε_y and $\varepsilon_{yc} =$ yield strain of the brace and column materials, respectively. The above equation is derived based on the assumption that axial displacements ($\delta_{hi,1}$ and $\delta_{hi,2}$) in the left and right columns are nearly same and the flexural deformations of columns and beams are negligible.

2.2 Design Displacement Profile

Design displacement profile for a framed structure can be determined from the expected lateral story drift at the inelastic stage. In most of the cases, the peak interstory drift response is noted at the first story levels of CBFs (Chao et al. 2013). Therefore, the first story drift (Δ_1) is considered as

the critical displacement for the selection of design displacement profile of CBFs. The design displacement (Δ_i) at ith story level is evaluated from the normalized inelastic mode shape of ith story (δ_i) as follows (Priestly et al. 2007):

$$\Delta_i = \delta_i\left(\frac{\Delta_1}{\delta_1}\right) \quad (2)$$

$$\delta_i = \left(\frac{H_i}{H_n}\right) \quad \text{for } n < 4 \quad (3a)$$

$$\delta_i = \frac{4}{3}\left(\frac{H_i}{H_n}\right)\left(1 - \frac{H_i}{4H_n}\right) \quad \text{for } n \geq 4 \quad (3b)$$

where, $n =$ number of stories, $H_i =$ Height from base to the ith level, and $H_n =$ Height from base to roof level. Displacement ductility is computed as the ratio of design (target) displacement to the yield displacement.

2.3 Development of Equivalent SDOF System

The first basic step involved in DDBD procedure is the substitution of MDOF structure to an equivalent SDOF system

Fig. 2 **a** Sway displacement and **b** rigid-body rotation of ith story of a braced frame
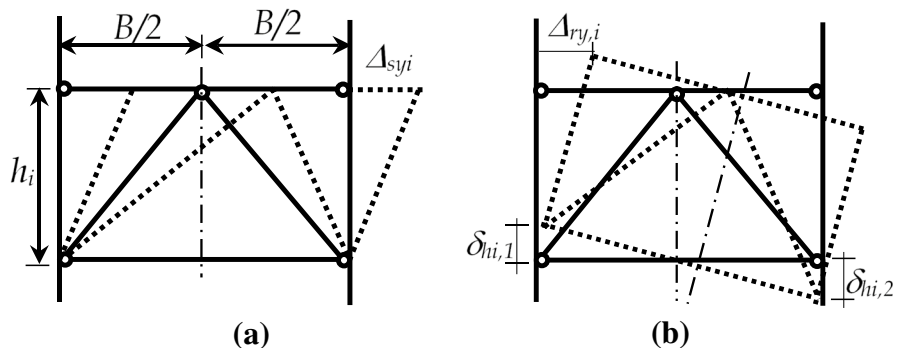
based on first inelastic mode of response. Effective mass (m_e), effective stiffness (K_e), equivalent design displacement ($\Delta_{d,e}$), and equivalent yield displacement ($\Delta_{y,e}$) for the equivalent SDOF system can be related to the story mass (m_i) and displacement (Δ_i) of the MDOF system as follows:

$$m_e = \frac{\sum_{i=1}^n m_i \Delta_i}{\Delta_d} \quad \Delta_{d,e} = \frac{\sum_{i=1}^n m_i \Delta_i^2}{\sum_{i=1}^n m_i \Delta_i} \quad \Delta_{y,e} = \frac{\sum_{i=1}^n m_i \Delta_{y,i}^2}{\sum_{i=1}^n m_i \Delta_{y,i}} \tag{4}$$

Design displacement ductility factor, μ of the equivalent SDOF structure can be given by

$$\mu = \frac{\Delta_{d,e}}{\Delta_{y,e}} \tag{5}$$

EVD coefficient of the equivalent SDOF system can be determined from the non-dimensional brace slenderness ratio (λ) and displacement ductility (μ) of CBFs as follows (Wijesundara et al. 2011):

$$\xi_{CBF} = 0.03 + \left(0.23 + \frac{\lambda}{15}\right)(\mu - 1) \quad \text{for } \mu < 2 \tag{6a}$$

$$\xi_{CBF} = 0.03 + \left(0.23 + \frac{\lambda}{15}\right) \quad \text{for } \mu \geq 2 \tag{6b}$$

Wijesundara et al. (2011) recommended the lower and upper limits of λ as 0.4 and 1.6, respectively. The minimum value of ζ_{CBF} can be computed as 28.7% using above equations. However, Salawdeh and Goggins (2013) found that using actual values of λ even outside of this range resulted in the reasonably accurate prediction of EVD. Hence, in this study, above expressions for EVD are assumed to be valid for any value of λ. The determination of λ for the MDOF system requires an iterative procedure. In the design process, a value of λ is assumed for the equivalent SDOF system and braces are sized accordingly for the calculated lateral forces corresponding to obtained the base shear (discussed later). The process is repeated until the average of value of λ for the MDOF system is found to be equal to the assumed value for the SDOF system.

2.4 Computation of Design Base Shear

Displacement response spectrum for 5%-damping can be scaled to determine the design displacement for the computed EVD as follows (Eurocode 8, 2009):

$$S_{d,\xi} = S_{d,5\%} \left(\frac{7}{2 + \xi}\right)^{0.5} \tag{7}$$

where, $S_{d,5\%}$ and $S_{d,\xi}$ are, respectively, the displacement spectra corresponding to 5% and ξ% of critical damping.

Design base shear force for MDOF structure can be obtained from the equivalent of SDOF system as follows:

$$V = K_e \Delta_d \quad K_e = \frac{4\pi^2 m_e}{T_e^2} \tag{8}$$

The distribution of base shear along the height of structure should be based on the proportion of mass and displacement at different floor levels. For the low-rise frames with nearly-uniform story mass distribution over the height, lateral seismic force (F_i) at any story level can be determined using the following expression (ASCE 7-10, 2010):

$$F_i = \frac{w_i H_i^k}{\sum_{j=1}^n w_j H_j^k} V \tag{9}$$

where w_i and H_i are the effective seismic weight and height measured from base to ith level, respectively, and k is an exponent linearly varying from 1 to 2 depending on the structure period between 0.5 to 2.5 s. Time period (T) of structure can be obtained as follows (ASCE 7-10, 2010):

$$T = T_a = C_t h_n^x \tag{10}$$

where, the values of C_t and x are 0.0488 and 0.75 for CBFs, respectively, and h_n (m) is the height measured from the base to the highest level of the structure.

2.5 Design of Members

The design of braces at each story is governed by the maximum compressive force acting on the brace members due to earthquake and gravity loads. Assuming the braces arranged in chevron configuration would resist equal story shear, axial compressive force (C_i) in each brace due to seismic and gravity loads can be determined using the following expression:

$$C_i = \frac{V_{fi}}{2\cos\alpha_i} + \frac{1}{\sin\alpha_i}\left(\frac{5w_G l}{16}\right) \tag{11}$$

where, V_{fi}= story shear, w_G= uniformly distributed gravity load on beam of length, l. An iterative procedure is followed to determine the final brace sizes so as to match the non-dimensional slenderness ratio of braces with the assumed value for the SDOF system. The performance goals of no brace fracture during DBE level events and delayed brace fracture during MCE level events may be accomplished by restricting the peak interstory drift and imposing the width-to-thickness ratio limitation on constituent members. AISC 341-10 (2010) requires that columns and braces of an SCBF should be highly ductile members while beam members should be moderately ductile.

Design of beams, columns and connections can be carried out using capacity design approach. Beam sizes are determined for the expected ultimate demand from braces in tension and compression considering the pre-buckling and post-buckling stages. Figure 3 shows the free-body diagram of beam with pinned ends subjected to brace forces and gravity loading. The expected brace tension strength (T_i) is taken as $R_y F_y A_{g,i}$ whereas the expected pre-buckled and post-buckled compression strength (C_i) of brace are taken as $1.14 F_{cr} A_{g,i}$ and $0.3 F_{cr} A_{g,i}$, respectively, whereas, R_y is material overstrength factor, F_y is the material yield stress, F_{cr} is the critical buckling stress of brace, and $A_{g,i}$ is the gross cross-section area of braces. Axial force (C_b) and bending moment (M_b) demand on beams of CBFs can be estimated using following expressions:

$$C_{b,i} = T_{i+1} \cos \alpha_{i+1} + 0.5 F_i \qquad (12)$$

$$M_{b,i} = \left(T_i - C_i'\right) \sin \alpha_{i+1} \frac{l}{4} + \frac{w_{G,i} l^2}{8} \qquad (13)$$

Thus, beams are designed as beam-columns for combined axial force and uniaxial bending. The compressive force in a column of ith story is the sum of gravity loads ($C_{col,G,i}$), cumulated vertical component of compression brace capacity and half the net vertical resultant of the brace loads acting at mid-span of the beams and is given by:

$$C_{col,i} = C_{col,G,i} + \sum_{j=i+1}^{n} C_j' \sin \alpha_j + \sum_{j=i}^{n} \left(T_j - C_j'\right) \sin \alpha_j \qquad (14)$$

3 Design of Study Frames

In this study, direct displacement-based design methodology as discussed above has been applied to two example CBFs in order to verify their adequacy in exhibiting the desired seismic response. The details of section sizes, numerical modelling and selection of ground motions are discussed in the following sections.
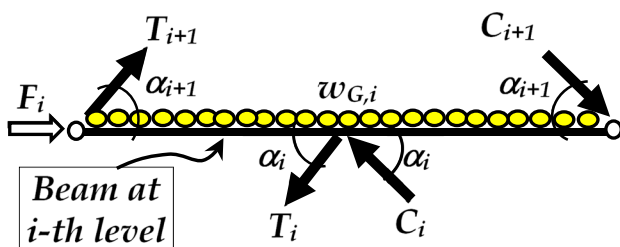

Fig. 3 Free-body diagrams illustrating forces acting on beam of a CBF

3.1 Determination of Section Sizes

3- and 6-story building frames with braces arranged in chevron configuration are considered in this study. These frames were previously designed by Sabelli (2000) using the NEHRP design spectra (FEMA 273 1997) and henceforth, are referred as 3V-NEHRP and 6V-NEHRP frames. The effective seismic weights for 3-story structure were 9390, 9390 and 10,159 kN for first to third floors. The corresponding values for 6-story structure were 9906, 9732, 9732, 9732, 9732, and 10,493 kN for the first to sixth floors. Both buildings are assumed to be located in downtown Los Angeles area with site class D. The 3V-DDBD and 6V-DDBD frames are designed for the maximum displacement arising out of two-hazard level cases for respective performance objectives i.e., 1.5% first story drift for DBE displacement spectrum and 3% first story drift for MCE displacement spectrum. The design DBE displacement response spectrum is obtained using the spectral response parameters based on FEMA 273 (1997) recommendations for the reference frames. For obtaining the MCE design, displacement spectrum provisions of ASCE 7-10 (2010) were compiled for obtaining the 'Risk-Targeted Maximum Considered (MCER) Response Spectrum'. NEHRP frames were designed for a response modification factor (R) of 6. All seismic forces were assumed to be resisted by the frames in braced bays only. All other frames were considered as gravity load-resisting frames. Design base shear for 3V-NEHRP and 6V-NEHRP frames are 3360 and 4590 kN, respectively (Chao et al. 2013).

Both these frames are designed using DDBD procedure as explained in the previous sections. Table 1 summarizes the yield and design displacement profiles of the study frames designed as per DDBD methodology. Material yield stresses of braces and columns/beams are considered as 317 and 345 MPa, respectively. The corresponding values of ε_y and ε_{yc} are computed as 0.158 and 0.172%. The angle of inclination (α) for the braces can be computed from width and height of a particular story. Assuming β equals to 0.75 in Eq. (1), the design displacement values are computed at different stories of 3- and 6-story frames. The values of m_e, $\Delta_{y,e}$ and $\Delta_{d,e}$ for the equivalent SDOF system are computed using the effective seismic mass values. EVD values for the 3- and 6-story frames are computed as 18.7 and 21.2%, respectively, for the converged values of normalized brace slenderness ratio. Design displacement spectrum is developed using the design spectral acceleration corresponding to short-period (S_{DS}) and one-second (S_{D1}) as 1.395 and 0.77 g (ASCE 7-10, 2010) as shown in Fig. 4. Design base shear for 3V-DDBD and 6V-DDBD frames are computed as 4249 and 6024 kN, respectively. Lateral forces at different story levels are obtained by distributing the design base shear along the height of frames using Eq. (9). It is worth mentioning that

Table 1 Summary of yield and design displacement profiles of the study frames

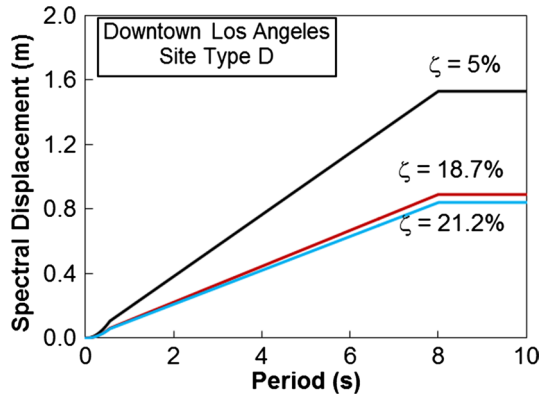| Story	3V-DDBD						6V-DDBD					
	h_i (m)	$\Delta_{sy,i}$ (m)	$\Delta_{ry,i}$ (m)	$\Delta_{y,i}$ (m)	$\delta_{,i}$	$\Delta_{d,i}$ (m)	h_i (m)	$\Delta_{sy,i}$ (m)	$\Delta_{ry,i}$ (m)	$\Delta_{y,i}$ (m)	$\delta_{,i}$	$\Delta_{d,i}$ (m)
6	–	–	–	–	–	–	3.96	0.013	0.0044	0.01714	1.00	0.3009
5	–	–	–	–	–	–	3.96	0.013	0.0044	0.01714	0.88	0.2670
4	–	–	–	–	–	–	3.96	0.013	0.0044	0.01714	0.76	0.2282
3	3.96	0.0127	0.0044	0.0171	1.00	0.1783	3.96	0.013	0.0044	0.01714	0.61	0.1845
2	3.96	0.0127	0.0044	0.0171	0.67	0.1189	3.96	0.013	0.0044	0.01714	0.45	0.1359
1	3.96	0.0127	0.0044	0.0171	0.33	0.0594	5.49	0.018	0.0085	0.02621	0.27	0.0823

Fig. 4 Design displacement response spectrum

the lateral force distribution profile for 6-story frame based on the proportion of mass and design displacement is found to be nearly same as that obtained using Eq. (9).

An overstrength factor (R_y) of 1.1 has been assumed to compute the expected yield strength of material. Effective length factor (K) is assumed as 0.85 for the out-of-plane buckling of braces (Lee and Goel 1990). In order to prevent premature brace fractures in the event seismic loading, braces of DDBD frames are chosen considering the brace fracture life (N_f) greater than 100 (Goel and Chao 2008). The value of N_f for HSS brace member largely depend on the compactness ratio as the slenderness ratio and is computed using the following empirical expression (Tang and Goel 1987):

$$N_f = \begin{cases} 262\dfrac{(b/d)(KL/r)}{\left(\frac{b-2t}{t}\right)^2} & \text{for } \dfrac{KL}{r} > 60 \\ 262\dfrac{(b/d)60}{\left(\frac{b-2t}{t}\right)^2} & \text{for } \dfrac{KL}{r} \leq 60 \end{cases} \quad (15)$$

where d is the overall depth of section, b is the overall width of section, t is the wall thickness, KL/r is the brace slenderness ratio. Brace compactness ratio represented by $(b - 2t)/t$ is limited to $0.64\sqrt{(E/f_y)}$ where, E is the Young's Modulus

and f_y is the material yield stress of braces (Goel and Chao 2008).

Design of columns has been carried out for the demand arising from the expected strength of brace tension and compression forces and beam forces. Since the beam-to-column connections are assumed to be pinned, the influence of bending strength of beams is negligible on columns. Hence, as a common practice, columns are designed only for axial load demands without considering the flexural action. Accordingly, column sections of DDBD frames required to satisfy the axial load demand are found to be same or even smaller than those for NEHRP frames. Figure 5 shows the structural sections used as braces, beams and columns of the DDBD and NEHRP frames considered in this study.

3.2 Computer Modelling

Seismic performance of the study frames is investigated numerically using a computer software *OpenSEES* (McKenna et al. 2007). Two-dimensional line-based models are developed for both NEHRP and DDBD frames. Simulation of inelastic deformation in the event of brace buckling has been realised by using ten number non-linear force-based beam-column elements per brace. Initial geometric imperfection in braces is assumed to be parabolic in shape with a central imperfection equal to one-thousandth of effective length. Each element had three integration points and the cross section has four elements each along the width and depth of braces. Co-rotational geometric transformation is used to model large deformation in the global response. *Steel02* material available in *OpenSEES* framework (which is basically a uniaxial Giuffre–Menegotto–Pinto steel material with isotropic strain hardening) is wrapped with fatigue material (Uriz et al. 2008) to simulate effects of low-cycle fatigue of braces. Beams and columns are modelled with force-based non-linear beam-column elements with three integration points per element.

P-Delta geometric transformation is used for the global co-ordinate system. Gusset plates are modelled as zero-length non-linear beam-column elements made of *Steel02*
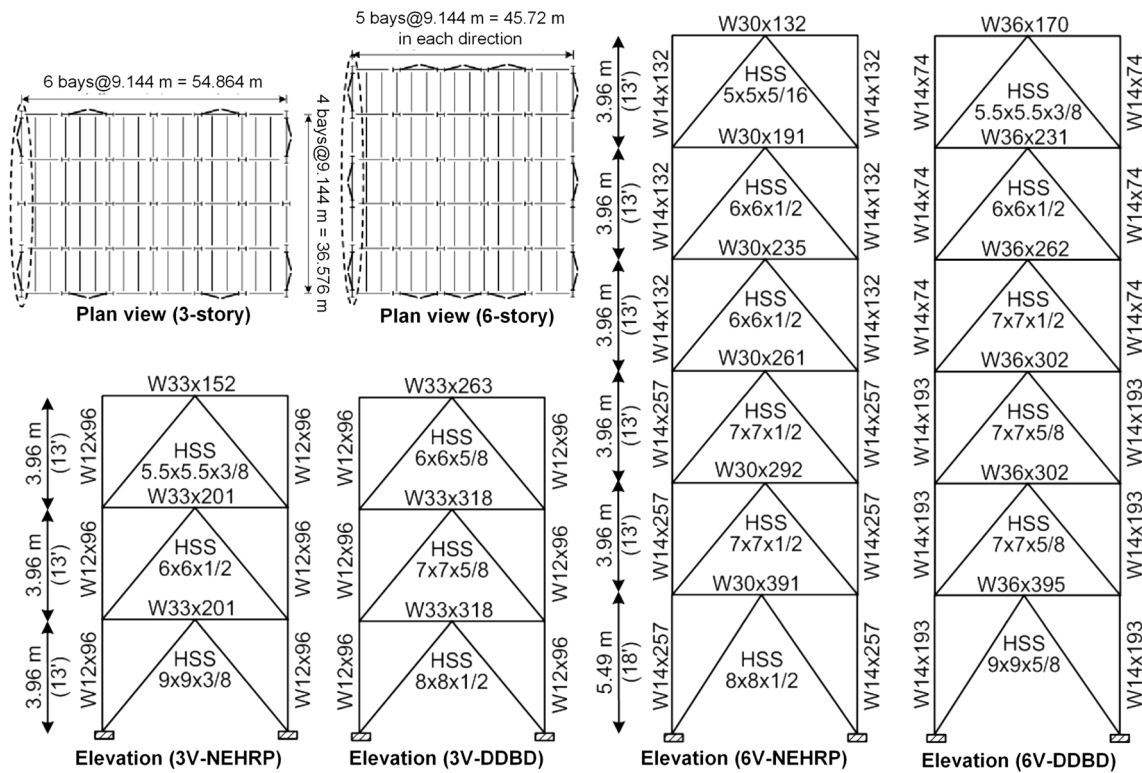
Fig. 5 Plan and elevation view of 3-story and 6-story study frames considered in this study

material with two integration points and co-rotational geometric transformation. Member ends at the gusset plate connections are defined as uniaxial rigid elastic elements modelled with large values of cross-sectional area and moment of inertia. Leaning columns with rigid links are modelled to capture the P-Delta effects due to gravity load. Rigid links are modelled as truss elements associated with large areas and moment of inertias to represent all the gravity beams and to have sufficient axial rigidity. Shear tabs (pinned connection) between the rigid links and braced frame beams are modelled by imposing constraint of equal horizontal and vertical displacement between the two connecting nodes while leaving the planar moment to be independent for two portions (i.e., free rotation). Ghost trusses, very small stiffness rotational truss elements, are applied between nodes on gusset plate ends of braces to diminish the convergence problems. Further, rigid truss elements with large areas are used to ensure that the beam nodes move horizontally together to model diaphragm effect of slabs. The supports of braced frame columns are defined as fixed, whereas in-plane rotation is allowed at the supports of gravity and leaning columns.

3.3 Selection of Ground Motions

Forty ground motions originally developed by Somerville et al. (1997) are considered for the nonlinear time-history analyses of the study frames in this study. Ground motions LA01 to LA20 correspond to the DBE hazard level with a 10% of probability of exceedance in 50 years, whereas the ground motions LA21 to LA40 represent the MCE hazard level with a 2% of probability of exceedance in 50 years. Some variation is noted in the average spectral plot of DBE ground motions and the design displacement spectrum. Therefore, these twenty ground motions are scaled, each with a suitable scale factor in order to fairly match the mean response spectrum with the design spectrum. These scale factors are obtained through a trial and error process by minimising the root mean square of the difference between the mean and the design spectra. However, no scaling of MCE ground motions (LA21-40) has been carried out in this study. Figure 6 shows the comparison of the mean displacement spectrum of DBE and MCE ground motions and the corresponding 5%-damped design spectrums. The selected ground motions representing MCE hazard level are relatively stronger than the required ones.

Fig. 6 Comparison of displacement spectra for 5% damping **a** DBE and **b** MCE levels
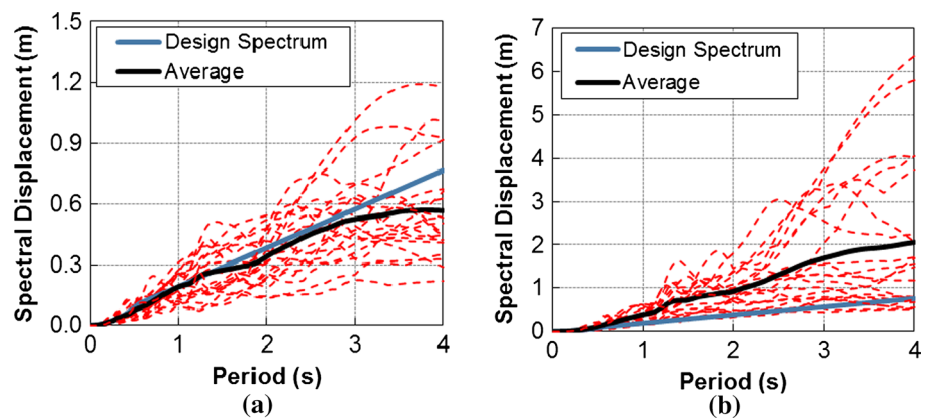
4 Results

Nonlinear time-history (NLTH) analyses are carried out for the selected ground motions. Stiffness and mass proportional Rayleigh damping is used with the damping coefficients calculated using the first and third natural frequencies. The value of tangent stiffness proportional damping assumed is 3% and Newmark acceleration-time integration scheme with beta and gamma as 0.5 and 0.25 is adopted in the dynamic analyses. The main parameters investigated are peak interstory drift ratio, residual inter-story drift ratio, hinge mechanism, and low-cycle fatigue damage of braces. FEMA 356 (2000) provides the indicative limiting values of transient inter-story drifts of 1.5 and 2% for braced steel frames for 'Life Safety' (LS) and 'Collapse Prevention' (CP) performance levels, which is linked to DBE (or BSE-1) and MCE (or BSE-2) level events, respectively. The respective values for residual interstory drifts are specified as 0.5 and 2%. To restrict the progressive structural damage and hence, cost of rehabilitation after a DBE event, limitation of no brace fracture and columns and beams remaining elastic are adopted as the desired yield mechanism for DBE hazard level. Braces may undergo extensive yielding and buckling cycles without fracture. For the MCE event, the prevention of structural collapse is the primary performance objective to be achieved by delaying the brace fracture.

4.1 DBE Analysis

The mean values of peak story shear, peak story displacements, peak inter-story drift ratio (ISDR) and peak residual interstory-drift ratio (RIDR) response of the study frames under the selected ground motions are considered for the comparison in this study. Figure 7 shows the variation of mean values of these parameters over the height of 3-story and 6-story frames under the DBE level ground motions. As compared to the NEHRP frames, both 3V-DDBD and 6V-DDBD frames exhibited the higher overstrength as compared to the design story shear. A higher overstrength

at the bottom story level is noted for 6V-DDBD frame as compared to the 6V-NEHRP frame. However, the difference in overstrength is reduced at the top story levels of the 6-story frames. Peak story shear capacity of 3V-DDBD and 6V-DDBD frames are noted as 9909 kN and 15,733 kN, respectively. 3V-DDBD exhibited the smaller story displacement as compared to the 3V-NEHRP frame, whereas both 6V-DDBD and 6V-NEHRP frames exhibited the nearly-same story displacements at the top story levels. In both cases, the peak values of story displacement are smaller than the design values. The peak values of ISDR for DDBD frames are noted as 0.81 and 0.79% as compared to 1.00 and 0.96% for the respective NEHRP frames of 3-story and 6-story formations, respectively. These values are found to be within the limiting ISDR value of 1.5% under DBE hazard level. The peak values of RIDR are reduced to 0.19 and 0.18% for 3V-DDBD and 6V-DDBD frames, respectively, as against the target value of 0.5% and also remained lesser than the corresponding NEHRP frames.

The mean story displacement profiles obtained from the DBE analysis of 3-story and 6-story frames as shown in Fig. 7 are noted to be different from those used in the design. This difference may be attributed to the following reasons: (a) The same column sections are used in three consecutive stories as followed in the practice, whereas the demand in columns in top stories would be significantly smaller than the capacity of provided sections; (b) The distribution of base shear over the height of frames is carried out as per current code of practice, which may not be exactly same as the design displacement profile. Hence, the average values of story displacements of the 3-story and 6-story DDBD frames under DBE ground motions are found to be conservative as compared to those corresponding to the design displacement profiles. However, the mean plus standard deviation (84 percentile) displacement profiles obtained from the peak story displacements showed a relatively better match with the design profile.

The proximity of brace failure is monitored during the analysis by incorporating a modified rain-flow cycle

Fig. 7 Comparison of story
shear, story displacement, ISDR
and RIDR response of **a** 3-story
and **b** 6-story CBFs under DBE
level ground motions
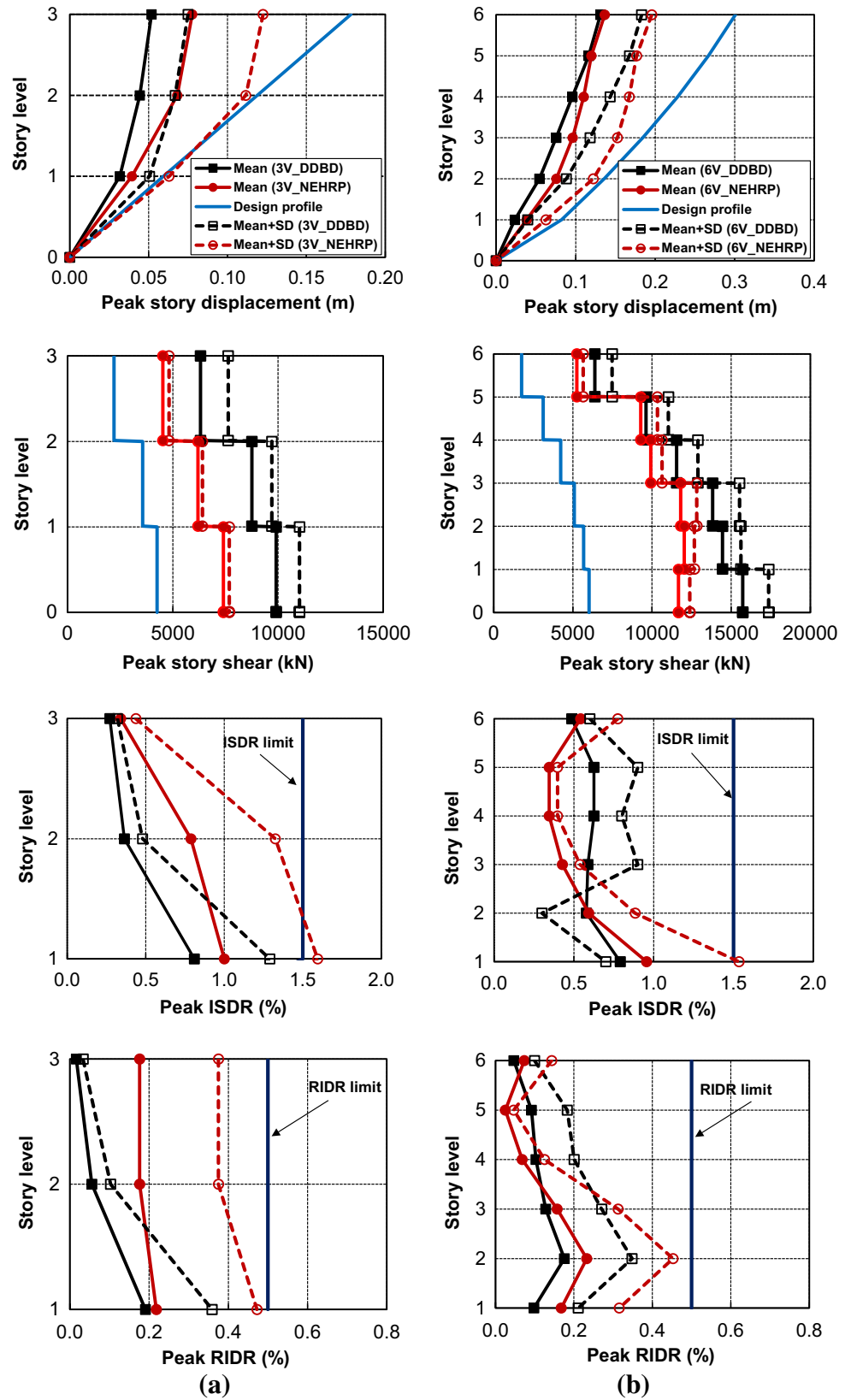
counting algorithm for incrementing and accumulating damage under low-cycle fatigue in the material models. Damage index (DI), calculated using Miner's rule, represents accumulated damage (0 for no damage as in virgin material and 1 for damage at fracture). The element stress-strain

Fig. 8 Comparison of brace damage index for **a** 3-story and **b** 6-story CBFs designed as per DDBD and NEHRP procedures under DBE level ground motions

relationships vanish when fatigue life is exhausted, i.e., DI = 1. Figure 8 shows the comparison of damage index for braces of DDBD and NEHRP 3-story and 6-story frames. Improved performance of DDBD frames is visible in the sense that no brace fracture is observed in DDBD frames, whereas NEHRP frames witnessed three cases of brace fracture in the DBE ground motions. The average maximum brace damage indices observed are 0.28, 0.14, 0.43, and 0.21 for 3V-DDBD, 6V-DDBD, 3V-NEHRP and 6V-NEHRP frames, respectively.

Figure 9 shows the formation of plastic hinging in the study frames subjected to the DBE level ground motions. The average peak stresses remained below the inelastic range for both DDBD and NEHRP frames in the DBE excitations, matching the target performance. However, plastic hinge formation at the base of first story columns is observed in six and nine cases of DBE time history for 3V-DDBD and 3V-NEHRP frames, respectively. For 6-story frames, plastic hinging occurred in fourth to sixth story columns in as many cases for the two design frames.. From the above results, it is clear that DDBD frames met all the performance objectives for DBE ground motions and their performance is superior than NEHRP designed structures in respect of all studied parameters.
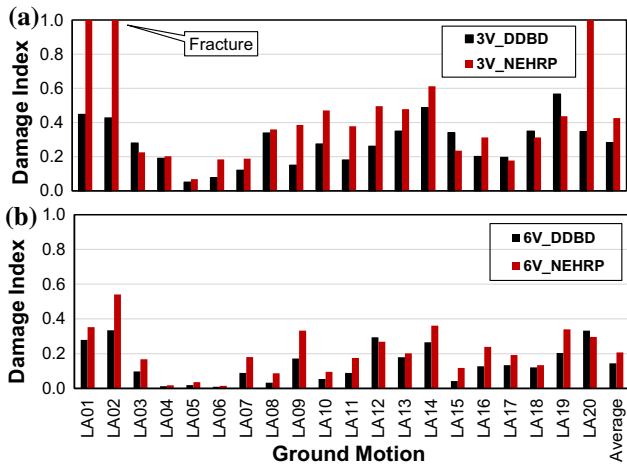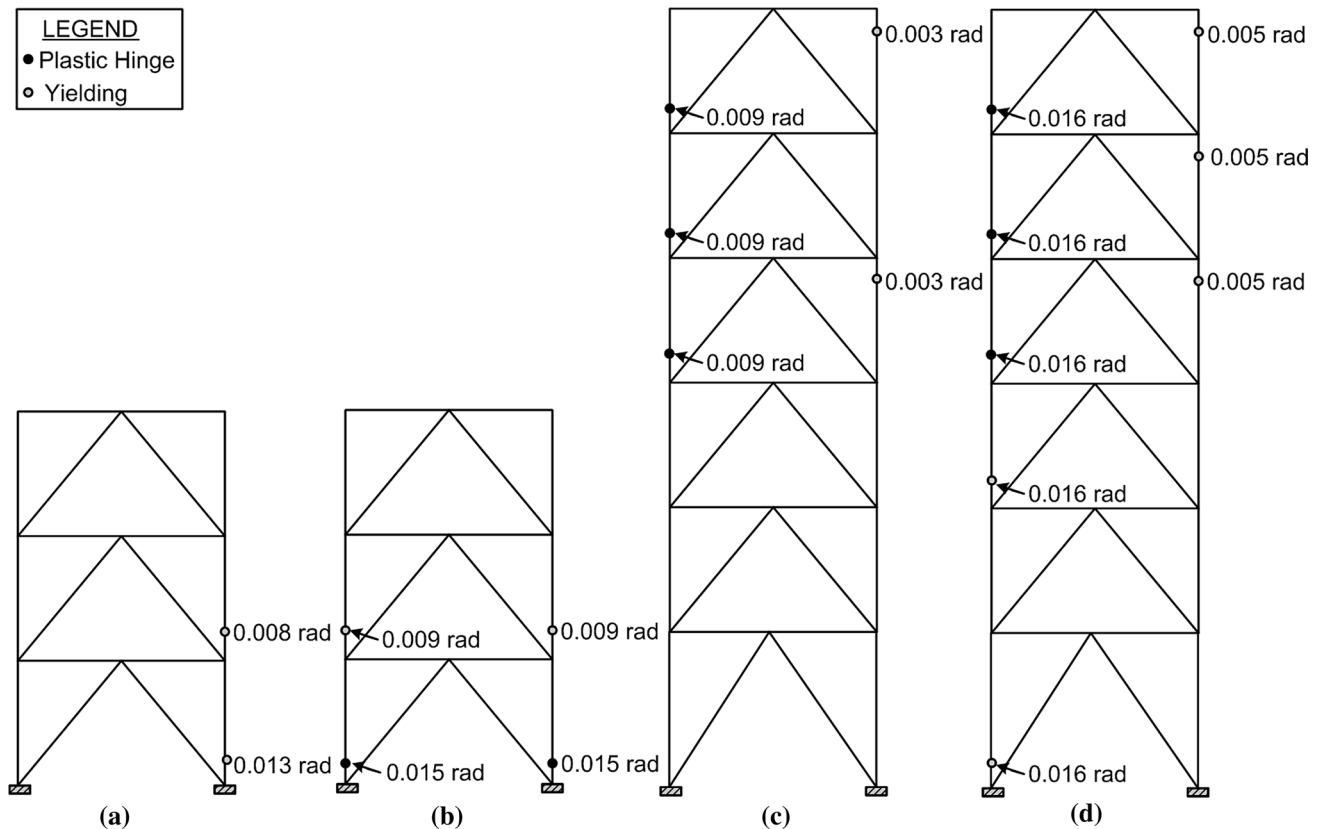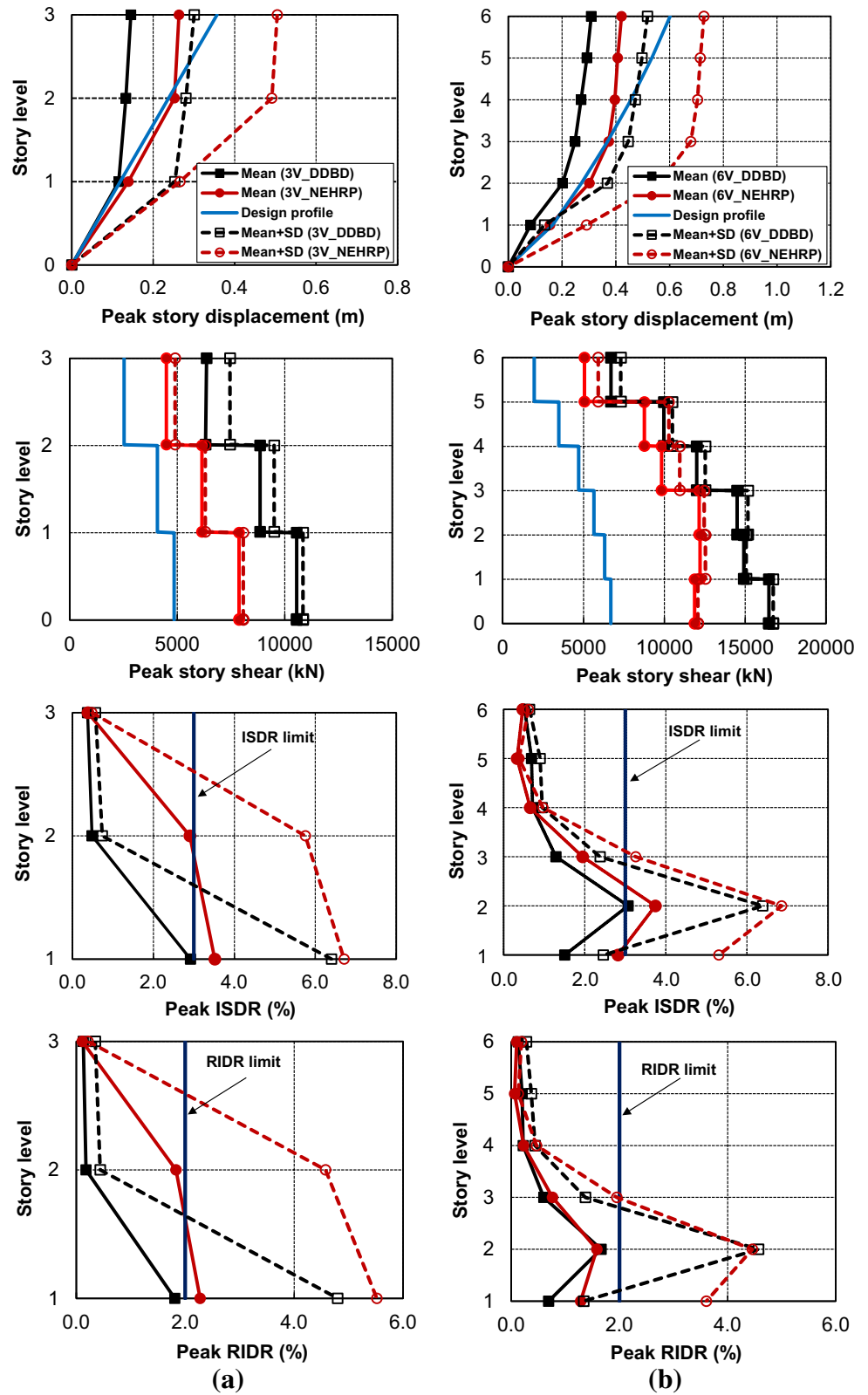

Fig. 9 Comparison of plastic hinges formed in study frames **a** 3V-DDBD, **b** 3V-NEHRP, **c** 6V-DDBD, and **d** 6V-NEHRP

Fig. 10 Comparison of story shear, story displacement, ISDR and RIDR response of **a** 3-story and **b** 6-story CBFs under MCE level ground motions

4.2 MCE Analysis

Figure 10 shows the variation of story shear, story displacement, ISDR and RIDR response of both 3- and 6-story frames under the MCE level ground motions. The peak story displacements of DDBD frames are observed to be lesser than those of NEHRP frames and within the design values for both 3- and 6-story formations. The peak values of top story displacements are noted as 0.145 and 0.263 m against the design value of 0.357 m for 3V-DDBD and 3V-NEHRP frames. The corresponding values are noted as 0.308 and 0.420 m against the design value of 0.600 m for 6V-DDBD and 6V-NEHRP frames. Except at second story of 6V-DDBD frame, the peak ISDR values for DDBD frames remain within the design values. The NEHRP frames showed the higher drifts than DDBD frames particularly at the lower stories. The peak inter-story drifts at first story for DDBD frames are noted as 2.92 and 1.51% against and 3.52 and 2.82% for NEHRP frames as compared to the design inter-story drift of 3.00% for 3- and 6-story formations, respectively. Residual inter-story drift of DDBD frames is found to be smaller than the limiting value of 2%, for example, 1.81 and 0.69% at first story of 3V-DDBD and 6V-DDBD frames, respectively. In NEHRP frames, the residual drift exceeded the limiting value by 13.5% (2.27% observed average of non-collapse cases) at first story of 3-story frame. The RIDR value for the 6-story NEHRP frame is 1.60%, which is significantly higher than that of the DDBD frame.

DDBD frames (3V-DDBD and 6V-DDBD) witnessed collapse in the lesser number of ground motions (i.e., three collapse cases each) as compared to the 3V-NEHRP and 6V-NEHRP frames (i.e., six and four cases of collapse). The number of low-cycle fatigue brace fracture cases for DDBD frames were eleven each against fifteen and sixteen for the NEHRP frames of 3- and 6-story formations, respectively (Fig. 11). The DDBD frames performed better than their current-code designed counterparts (NEHRP) in terms of the smaller peak story displacement, the maximum and residual interstory drift and brace damage indices and higher peak story shear resisted for both 3-story and 6-story configurations. Considering the average results of non-collapse cases, the DDBD frames also met by and large the MCE level performance objectives of peak and residual inter-story drifts. The number of plastic hinges in the columns as well as their plastic rotations observed for DDBD frames were typically lesser than those for NEHRP frames. The primary objective of eliminating chances of structural collapse in strong MCE ground motions is largely achieved as the observed collapse cases were significantly reduced and may be perceived as extremely rare. Further, on one hand the peak story displacement, maximum and residual inter-story drift and brace damage
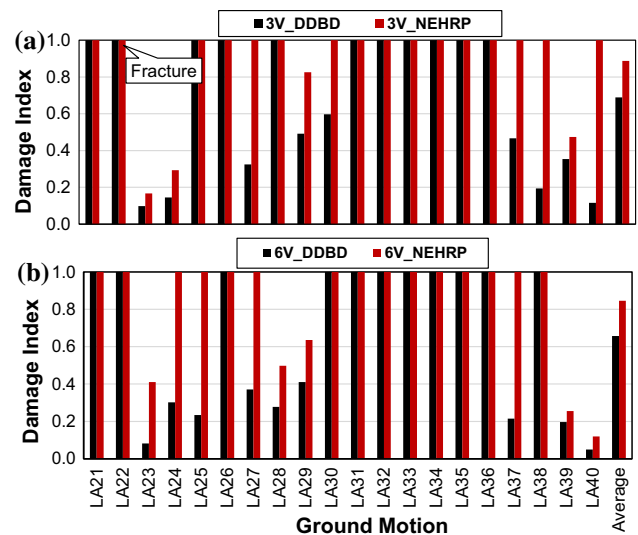

Fig. 11 Comparison of brace damage index for **a** 3-story and **b** 6-story CBFs designed as per DDBD and NEHRP procedures under MCE level ground motions

indices decreased and on the other hand peak story shear resisted by frames increased with the revised DDBD design. The DDBD frames also performed better than their current-code designed counterparts (NEHRP) in these parameters. Considering the average results of non-collapse cases, the DDBD frames also met by and large the MCE level performance objectives of peak and residual inter-story drifts. The damage in beams and columns marked by yielding and formation of plastic hinges is also considerably reduced.

Design base shear values for DDBD frames are found to be 20–30% higher than those of the NEHRP frames. This resulted in the relatively higher brace sections in the DDBD frames leading to the improved seismic performance. One of the important parameter used in the DDBD method is the normalized slenderness ratio (λ) of brace, which is used to determine the design base shear using the estimated value of equivalent viscous damping for the SDOF system. Brace sections in the mutli-story braced frame are selected in such a way that the average value of λ in all stories is nearly equal to that used in the computation of design base shear. This eliminated the possibility of any significant difference in brace strength and stiffness in consecutive stories and also avoided the drift concentration in a particular story level. Further, the selection of brace sections having the desired fracture life also reduced the vulnerability of brace failure under low-cyclic loading. These parameters led to the improved performance of DDBD frames as compared to the NEHRP frames.

5 Summary and Conclusions

A performance-based design procedure has been developed for conventional concentrically braced frames (CBFs) using direct-displacement based design (DDBD) approach. Performance objectives for the CBF structures are defined for two-level seismic hazard comprising of peak and residual inter-story drifts and structural damage, in terms of low-cycle fatigue damage of braces, yielding of columns and beams and structural failure. Two example CBFs 3- and 6-story are designed using the proposed methodology as well as current force-based code provisions. These frames are also subjected to same sets of ground motions and the NLTH results obtained are compared with those of DDBD frames.

Analysis results confirmed that CBFs designed with DDBD approach successfully attained the design displacement and drifts and result in conservative design in terms of high story shear capacities. The NLTH analyses results obtained confirmed capability of the proposed performance based-design process in imparting enough strength to the CBFs to meet target performance in DBE scenario and also improved performance than current code-based designed structure. Nevertheless the performance of DDBD frames was better than NEHRP frames in this case too. Although the process involves iteration in design for non-dimensional slenderness ratio, the process is fast converging and hence, quick and computational tools like spreadsheets may be easily implemented. The efficacy of this design procedure for high-rise CBFs may be investigated in the further research.

References

ANSI/AISC 341-10. (2010). *Seismic provisions for structural steel buildings*. Chicago, IL: American Institute of Steel Construction.

ASCE 7-10. (2010). *Minimum design loads for buildings and other structures*. Reston, VA: American Society of Civil Engineers.

Chao, S.-H., Karki, N. B., & Sahoo, D. R. (2013). Seismic behavior of steel buildings with hybrid braced frames. *ASCE Journal of Structural Engineering, 139*(6), 1019–1032.

Chopra, A. K. (1995). *Dynamics of structures: Theory and applications to earthquake engineering*. Upper Saddle River, NJ: Prentice Hall.

Della Corte, G, & Mazzolani, F. M. (2008). Theoretical developments and numerical verification of a displacement-based design procedure for steel braced structures. In *Proceedings of the 14th world conference on earthquake engineering*, Beijing.

Eurocode 8. (2009). *Design of structures for earthquake resistance—Part 1: general rules, seismic actions and rules for buildings,* EN 1998-1:2004/AC:2009, Brussels.

Fajfar, P. (1998). *Capacity spectrum method based on inelastic demand spectra*. IKPIR Report EE-3/98, University of Ljubljana, Slovenia.

Fajfar, P., & Gašperšič, P. (1996). The N2 method for the seismic damage analysis of RC buildings. *Earthquake Engineering and Structural Dynamics, 25*(1), 31–46.

FEMA 273. (1997). *NEHRP guidelines for the seismic rehabilitation of buildings*. Washington, DC: Federal Emergency Management Agency.

FEMA 356. (2000). *Pre-standard and commentary for the seismic rehabilitation of buildings* (p. 2000). Washington, DC: Federal Emergency Management Agency.

Ghobarah, A. (2001). Performance-based design in earthquake engineering: state of development. *Engineering Structures, 23,* 878–884.

Goel, S. C. & Chao, S. H. (2008). P*erformance-based plastic design-earthquake resistant steel structures*. International Code Council.

Goggins, J. G., & Sullivan, T. J. (2009). Displacement-based seismic design of SDOF concentrically braced frames. In F. Mazzolani, J. M. Ricles & R. Sause (Eds.), *STESSA 2009* (pp. 685–692). Milton Park: Taylor & Francis Group.

Kumar, P. C. A., & Sahoo, D. R. (2016). Optimum range of slenderness ratio of HSS braces for special concentric braced frames. *Advances in Structural Engineering, 19*(6), 928–944.

Kumar, P. C. A., Sahoo, D. R., & Kumar, N. (2015). Limiting values of slenderness ratio for circular braces of concentrically braced frames. *Journal of Constructional Steel Research, 115,* 223–235.

Lee, H.-S., & Goel, S. C. (1990). *Seismic behavior of steel built-up box shaped bracing members and their use in strengthening reinforced concrete frames*. Rep. No. UMCE 90-7, Dept. of Civil and Environmental Engineering, Univ. of Michigan, Ann Arbor, MI.

McKenna, F., Fenves, G. L., Jeremic, B., & Scott, M. H. (2007). *Open system for earthquake engineering simulation (OpenSEES)*. Berkeley, CA: University of California.

O'Reilly, G., Goggins, J., & Mahin, S. (2012). Performance-based design of a self-centering concentrically braced frame using the direct displacement-based design procedure. In *Proceedings of the 15th world conference on earthquake engineering*. Lisbon, Portugal.

Priestley, M. J. N. (2000). Performance-based seismic design. In *Proceeidngs of the 12th world conference on earthquake engineering*, Auckland.

Priestley, M. J. N., Calvi, G. M., & Kowalsky, M. J. (2007). *Displacement-based seismic design of structures* (p. 721). Pvia: IUSS Press.

Sabelli R. (2000). *Research on improving the design and analysis of earthquake resistant steel braced frames*. FEMA/EERI report, Federal Emergency Management Agency, Washington, DC.

Sahoo, D. R., & Chao, S.-H. (2010). Performance-based plastic design of buckling-restrained braced frames. *Engineering Structures, 32*(9), 2950–2958.

Sahoo, D. R., & Rai, D. C. (2013). Design and evaluation of seismic strengthening techniques for RC buildings with soft-story. *Engineering Structures, 56*(11), 1933–1944.

Salawdeh, S., & Goggin, J. G. (2012). Direct displacement based seismic design of multi-storey concentrically braced frame structures. *IABSE symposium report, global thinking in structural engineering: Recent achievements,* (Vol. 98, No. 1, pp. 1–8). International Association for Bridge and Structural Engineering.

Salawdeh, S., & Goggins, J. (2013). Numerical model for steel brace members incorporating brace members incorporating a fatigue model. *Engineering Structures, 46,* 332–349.

Somerville P. G., Smith M., Punyamurthula S., & Sun J. (1997). *Development of ground motion time histories for phase 2 of the FEMA/SAC steel project*. Report No. SAC/BD-97/04, Sacramento, CA.

Tang, X., & Goel, S. C. (1987). *Seismic analysis and design considerations of braced steel structures*. Report No. UMCEE 87-04,

Department of Civil Engineering, University of Michigan, MI, USA.

Tremblay, R. (2002). Inelastic seismic response of steel bracing members. *Journal of Constructional Steel Research, 58,* 665–701.

Uriz, P., Filippou, F. C., & Mahin, S. A. (2008). Model for cyclic inelastic buckling of steel braces. *ASCE Journal of Structural Engineering, 134,* 619–628.

Wijesundara, K. (2009). *Design of concentrically braced steel frames with RHS shape braces*. Doctoral thesis, European Centre for Training and Research in Earthquake Engineering (EUCENTRE), Pavia, Italy.

Wijesundara, K. K. (2012). Seismic design of steel concentric braced frame structures using direct displacement based design approach. In *Proceedings of the 2nd international conference on sustainable built environments (ICSBE 2012)*, Sri Lanka.

Wijesundara, K. K., Nascimbene, R., & Sullivan, T. J. (2011). Equivalent viscous damping for steel concentrically braced frame structures. *Bulletin of Earthquake Engineering, 9*(5), 1535–1558.